Pergamon

PII: S0191-8141(96)00106-X

Journal of Structural Geology, Vol. 19, No. 5, pp. 673 to 685, 1997

0191-8141/97 $17.00 + 0.00

Effective tension–shear relationships in extensional fissure swarms, axial rift zone of northeastern Iceland

JACQUES ANGELIER and FRANÇOISE BERGERAT

Tectonique Quantitative, Département de Géotectonique (URA 1759 CNRS), Bte 129, T26-25 E1, Université P. et M. Curie, 4 pl. Jussieu, 75252 Paris, Cedex 05, France

OLIVIER DAUTEUIL

Géosciences Rennes (UPR 4661 CNRS), Campus de Beaulieu, Av. Général Leclerc, 35042 Rennes Cedex, France

and

THIERRY VILLEMIN

Laboratoire de Géodynamique (UPRESA 5025 CNRS), Université de Savoie, 73376 Le Bourget-du-Lac Cedex, France

(*Received* 25 *January* 1996; *accepted in revised form* 21 *November* 1996)

Abstract—The geometry of fracture systems in selected areas of the active Krafla fissure swarm, mid-Atlantic ridge, northeastern Iceland, is analysed. Based on geodetic analysis of the present-day topography at the top of Holocene basaltic lava flows which fill the axial rift zone, the deformation of this initially horizontal surface can be reconstructed. Extensional deformation is localised at all scales and block tilting, though present, remains minor. Using simple models of the surface expression of normal faults, the geometrical characteristics of the topographic features related to active deformation during tectonic–volcanic events are quantitatively analysed. At crustal depths of about 1 km, normal faults are present and have an average 70° dip. Comparison with the dip data of older normal faults observed in the uplifted and eroded shoulders of the rift zone, at palaeodepths of 1–2 km, indicates that this dip determination is valid. Comparisons between the local case study and structural analyses of active fissure swarms on a larger scale suggest that normal faulting plays a major role in the middle section of the thin, newly formed brittle crust of the rift zone. In the axial oceanic rift zone of NE Iceland, the extensional deformation in the upper crust is dominated by horizontal tension and shear of normal sense, their relative importance depending on depth. Absolute tension dominates in the uppermost several hundred metres of the crust, resulting in the development of fissure swarms. Effective tension plays an important role at a deeper level (2–5 km), because of the presence of magmatic fluid pressure from magma chambers which feed dyke injections. At crustal depths of about 1 km, normal shear prevails along fault planes which dip 60°–75°. This importance of normal shear at moderate depth, between upper and lower crustal levels where tension prevails, is pointed out. Within the extensional context of rifting, these variations of tectonic behaviour with depth are controlled by both the lithostatic pressure and the effective tension induced by the presence of magmatic fluid pressure. © 1997 Elsevier Science Ltd.

INTRODUCTION

Fissuring and tension crack development are the most common expressions of extensional tectonics at the Earth's surface. At crustal depths of few hundred metres to few kilometres, extension is commonly accommodated by normal faulting, as occurs along the mid-Atlantic ridge in the active oceanic rift zone of Iceland (Fig. 1a). Spectacular active crack opening, which occurs in the fissure swarms of the axial rift zone of Iceland, is related to volcano-tectonic activity (Gudmundsson, 1987a,b, 1995a; Opheim and Gudmundsson, 1989). Normal faulting at depth is indicated by structural geology studies (Saemundsson, 1980) and analyses of earthquake focal mechanisms (Einarsson, 1991). The transition from absolute tension characterised by fissure opening to shear characterised by normal faulting occurs at shallow depths in the axial rift zone of Iceland, so that the fractures are commonly subvertical at the surface but have dips between 60° and 75° at depths of several hundred metres (Gudmundsson and Bäckström, 1991; Forslund and Gudmundsson, 1991, 1992; Gudmundsson, 1992). In the volcanic context of the oceanic rift zone (Fig. 1b), tension crack opening also occurs at greater depths, because of magmatic pressure and related dyke injection (Gudmundsson, 1987a,b; Opheim and Gudmundsson, 1989).

The axial rift zone has been repeatedly filled by lava flows. Because of the fluid character of the basalts, the floor of this depression generally corresponds to a horizontal palaeosurface, mostly of Holocene age. The deformation of this surface, at the top of the most recent lava flows, is accommodated by fissuring and faulting, and localised at all scales. This deformation can be analysed using geodetic methods. Simple measurements provide data on the vertical offsets and the horizontal

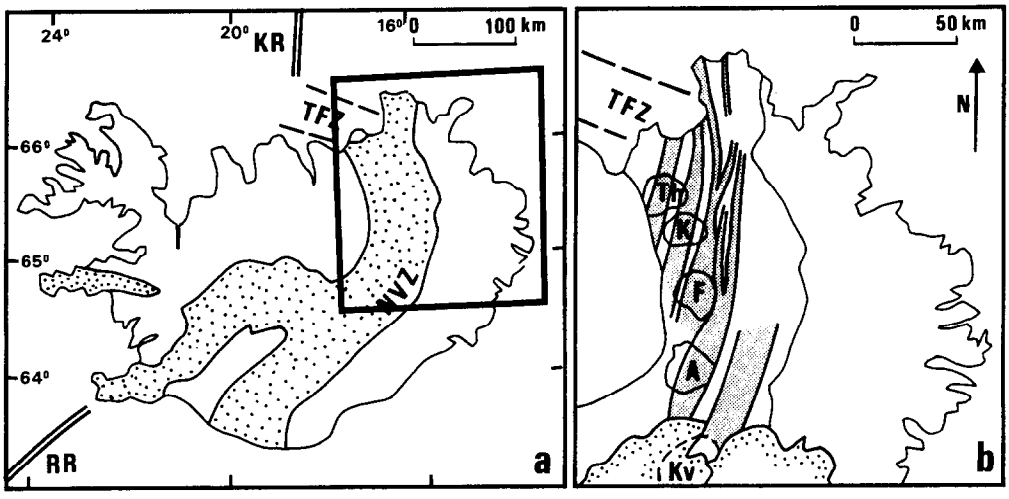

Fig. 1. The axial rift zone and fissure swarms of northeastern Iceland. (a) Location in Iceland, with rift zones dotted (KR, Kolbeinsey Ridge; RR, Reykjanes Ridge; NVZ, Neovolcanic Zone; TFZ, Tjörnes Fracture Zone) and box corresponding to (b). (b) Fissure swarms of northeastern Iceland (shaded, with associated central volcanoes shown: Th, Theistareykir; K, Krafla; F, Fremri-Namur; A, Askja; Kv, Kverkfjöll).

transverse opening of the fractures in the fissure swarms. Such analysis allows direct determination of the youngest extensional strain in the axial rift zone, where extension and the creation of oceanic lithosphere occur.

In this paper, extensional deformation at the surface is characterised in order to determine the geometry of the underlying normal fault systems. In the Krafla fissure swarm of NE Iceland (Fig. 1b), we analyse, with geodetic methods, the fracture pattern in a central segment of this fissure swarm. This segment is located near the Krafla central volcano, at the surface of a lava flow, 2000–2500 years old. The results of the geometrical reconstruction are compared with those provided by geological observations in the deeper, eroded sections of the flanks of the rift zone in Iceland.

THE KRAFLA FISSURE SWARM, ICELAND

At the divergent plate boundary in NE Iceland, the N–S-trending segment of the axial rift zone is approximately 200 km long and 60 km wide (Fig. 1). It consists of the so-called neo-volcanic zone where volcanic rocks younger than 0.7 Ma crop out and where seismic activity occurs (Saemundsson, 1980). Five large fissure swarms are present, trending NNE–SSW and forming an en échelon pattern. They are each 60–100 km long and 5–20 km wide (Fig. 1b).

The Krafla fissure swarm extends north and south of the Krafla central volcano (Fig. 1b), from the western edge of the axial rift zone, south of lake Myvatn to the eastern tip of the Tjörnes transform fault zone on the coast at Axarfjördur (Fig. 2a). Numerous fractures dissect the flat top surface of the recent lava flows that fill the axial rift zone (Fig. 2b). The rim of the caldera of the Krafla central volcano, with a diameter of 8–10 km (Fig. 2c), is indicated by a distinctive dacitic welded-tuff layer (Björnsson *et al.*, 1977). About 35 eruptions occurred during the Holocene, most of them originating in the caldera or in the adjacent mountain Namafjall (Björnsson *et al.*, 1977). The Krafla fissure swarm clearly dissects the late Pleistocene volcanic formations, including the olivine tholeiites of the 10,000 year-old shield volcano Theistareykir (Opheim and Gudmundsson, 1989).

Among 21 rifting events in the Krafla area between 1975 and 1984, nine events resulted in volcanic eruptions. The inflation and deflation of the magma chamber, as related to rifting episodes and fissure eruptions, has been studied in detail by Björnsson *et al.* (1977) and by Tryggvason (1980, 1984, 1986a). The earlier evolution of the Krafla fissure swarm is also known at several places (Fig. 2a). Earthquakes and basaltic fissure eruptions occurred in 1724–1729 near Myvatn (Grönvold, 1984; referred to in Opheim and Gudmundsson, 1989). Basaltic fissure eruptions also occurred 1500–2000 years ago near Kelduhverfi, in the northern segment of the Krafla fissure swarm (Eliason, 1979; referred to in Opheim and Gudmundsson, 1989). At a similar time, spatter cones connected to tectonic fractures developed near Gjastykki (Opheim and Gudmundsson, 1989).

One of the most spectacular active fracture patterns of the Krafla fissure swarm is in the Mófell–Hrutafjöll area, north of the Krafla (Fig. 2a). This complex area, which is not studied here, provides a good illustration of the morphological features in the active fissure swarm (Figs 3 & 4). The distribution of fractures was studied there by Opheim and Gudmundsson (1989): the average length of fractures is 350 m, and the predominant strike is N003°E–N018°E. No evidence of lateral displacement was found along these fractures, suggesting that the direction of extension averages N100°E, perpendicular to the trend of the fissure swarm. This is similar to the trend of the spreading vector in Iceland, which is N113°E

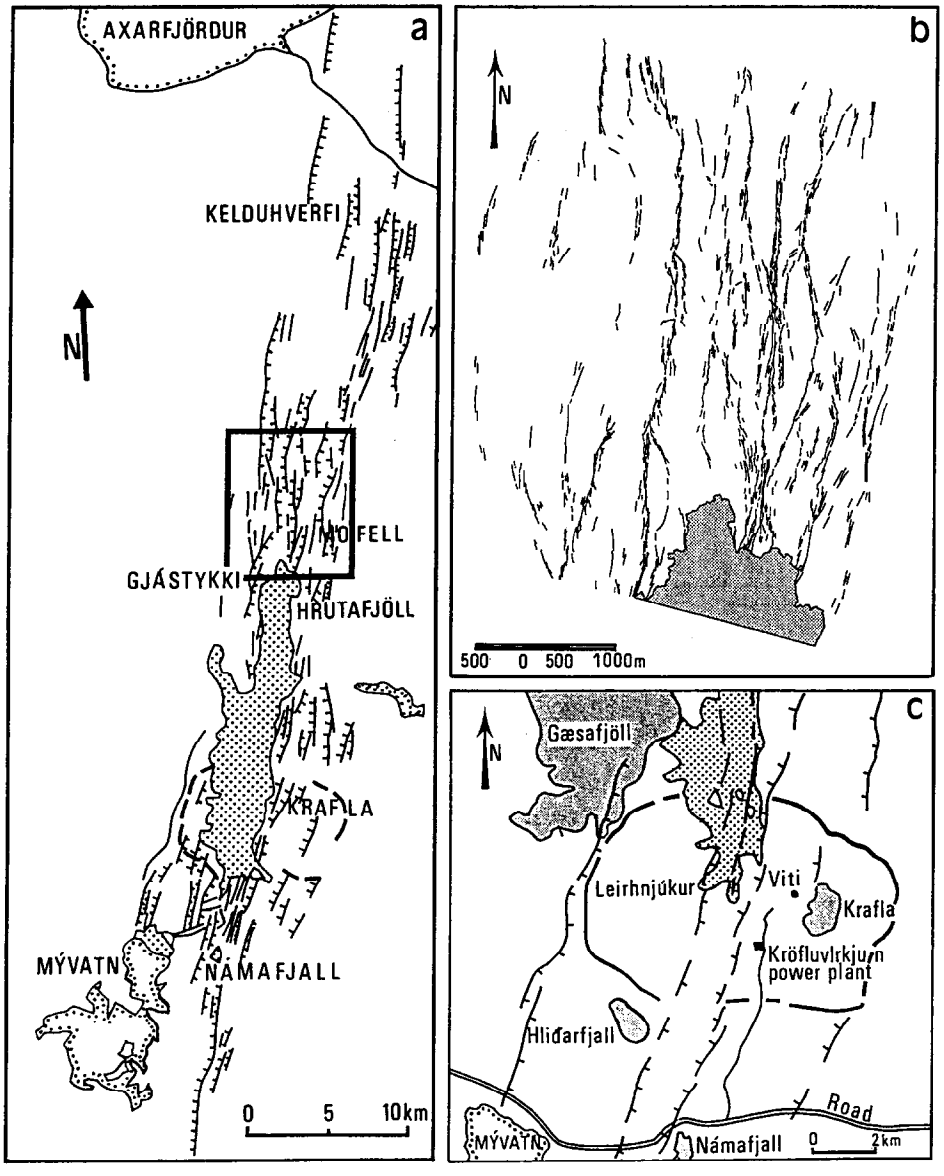

Fig. 2. The Krafla fissure swarm, northeastern Iceland. (a) General map of the fissure swarm between Myvatn and the northern coast, after Björnsson *et al.* (1984) and Opheim and Gudmundsson (1989). Pleistocene and Holocene volcanic rocks are left white, recent lava flows of 1724–1729 and 1975–1984 are dotted, fractures are thin lines with barbs on the downthrown side where vertical offsets are present and the thick dashed line indicates the rim of the Krafla caldera. Small frame shows location of (b). (b) Map of the fracture system in the Mófell–Hrutafjöll area, based on interpretation of aerial photographs, geodetic survey and field observation. (c) Map of the Krafla caldera area, after Gudmundsson (1986). Major volcanoes are shaded; 1975–1984 Krafla lava flows are dotted; the rim of the Krafla caldera is a thick line; normal faults are lines with barbs indicating the downthrown side.

according to Saemundsson (1974) and N100°E according to Saemundsson (1980) and De Mets *et al.* (1990).

The 1975–1984 rifting episode involved a total extension of 9 m across the fissure swarm at the northern margin of the Krafla caldera. At Hrutafjöll, the dilation was around 7 m (Gudmundsson, 1995b). The dilation decreased southward to zero south of lake Myvatn, and northward to 2 m on the coast at Axärfjordur (Tryggvason, 1984). The extension during the rifting events affected zones a few km wide within the fissure swarm. During the 1975–1984 rifting episode, the flanks of the fissure swarm underwent contraction by more than 0.3 m km^{-1} in some areas (Tryggvason, 1984). This amount should be substracted from the total fissure dilation while estimating the extension across the whole rift. Such a lateral contraction coeval with, and in the same direction as, axial fissure opening denoted the elastic behaviour of the upper crust.

Within the main recent fissure swarm (Fig. 2), N–S-trending faulted blocks, 1 km wide on average, are separated by major scarps which are likely to be the surface expression of normal faults (Fig. 3a). Because faulting affects Holocene lava flows and because erosion is minimal, the height of these scarps reflects the vertical offset, which ranges from 2.5 m to 16.8 m for the main faults. Each of these major scarps corresponds to a

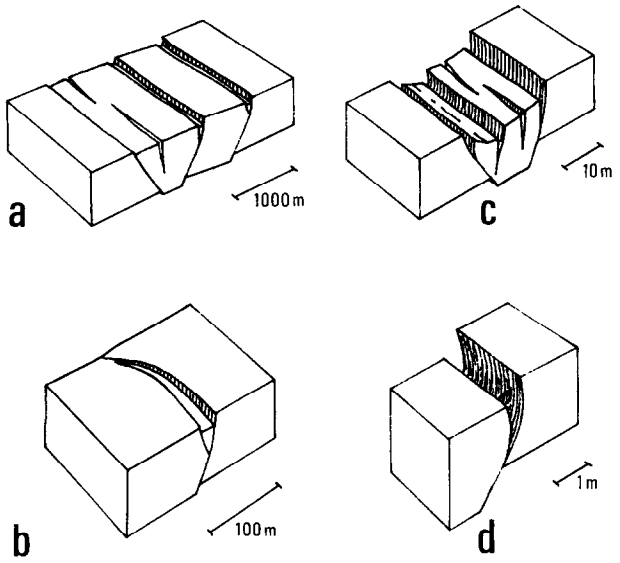

Fig. 3. Main types of fracture–fissure patterns at different scales, from examples in the Mófell–Hrutafjöll segment of the Krafla fissure swarm. (a) Large faulted-tilted blocks. (b) Major fault scarp with a graben-like structure (note the curvature at the end of the fault). (c) Detail of a graben-like structure, with fissures and block tilting inside the graben. (d) Minor open fissure with vertical offset.

graben-like structure, usually about 10–20 m wide (Fig. 3b & c). Such structures can be traced for up to 3 km, and commonly adopt an arcuate shape near their terminations (Fig. 3b): concavity faces the downthrown block, which is consistent with normal faulting. A graben-like structure may include several blocks, 1–10 m wide, often tilted and separated by fissures (Fig. 3c). Vertical tension fractures without any component of shear are present in the fissure swarm, but in many cases some vertical offset is also present, suggesting again that normal faulting plays a role (Fig. 3d).

New measurements in the Mófell area (Fig. 2a & b) provided average values of 8.1 m, 12.5 m and 2.5 m for the vertical offsets of the three major fault zones (from east to west) and of 5.5 m, 4.3 m and 9.6 m for the corresponding cumulative dilations. The dilation estimates were obtained by adding values measured across all individual fractures observed within each fault zone (with corrections taking the tilt into account where necessary), whereas the vertical offsets were obtained by geodetic means. These few preliminary estimates do not allow rigorous analysis of the deformation, but provide some basis for a geometrical comparison between the largest structures of the fissure swarm (Fig. 4a & b) and the smaller ones near the Leirhnjukur, which are described hereafter (Fig. 5). In addition to large structures, many minor fractures occur. Because they are numerous, their contribution to extension is significant (always more than 10%) and thus cannot be neglected in estimates of deformation rates. The complete geometrical analysis shown below (Leirhnjukur) includes consideration of all fractures and thus allows accurate reconstitution of the deformation, whereas in the Mófell area only the largest fault zones were analysed.

Figure 4 illustrates the different aspects of the extensional surface deformation in the Krafla fissure swarm. The pattern of fractures is visible on aerial photographs, at the scale of several kilometres (Fig. 4a, showing approximately the southeastern quarter of the area mapped in Fig. 2b). Tilted blocks and fissures are present in graben-like structures along the major scarps in the Mófell area, at the scale of several tens of metres in width and height (compare Fig. 4b with Fig. 3c). Small fissures with both horizontal dilation and vertical offset are common, at the scale of few decimetres or metres in width and height (compare Fig. 4c with Fig. 3d).

ANALYSIS OF A FRACTURE SYSTEM

A typical part of the Krafla fissure swarm has been studied. It is located near the centre of the Krafla caldera (Fig. 2c), 1.7 km west of the crater Viti and 1.7 km northwest of the geothermal power plant Kröfluvirkjun, at the southern tip of the volcanic hill Leirhnjukur. This area is of interest because it forms the western boundary faults of the Holocene, 1–2 km wide central graben that bisects the Krafla caldera and marks the axis of a wider graben zone in which the caldera is located (Fig. 2c).

Analysis of the fracture pattern in a 280 m long and 150 m wide area has been carried out. In this area, multiple fractures dissect the flat upper surface of a pile of the lava flows (Fig. 5). This lava flow (called Kröflu-halshraun) is probably about 10,000 years old (Saemundsson, 1991). The top surface of this lava flow forms a large flat area on the eastern side of Leirhnjukur. The fractures studied do not cut an aa lava flow of the 1975–1984 eruptions, coming from the north on the western side of Leirhnjukur. At the site studied, the aa lava flow (visible in Fig. 5) is part of the 1984 fissure eruption. All fractures are observable at the surface and most of them resemble the fracture shown in Fig. 4(c). Most of the area studied is seen in the photograph of Fig. 5, where the faulted late Holocene lava flow is covered with thin soil and thick grass whereas the lava flow of the 1984 eruption is black, without any vegetation. In addition, Fig. 5 shows the edge of a grey pahoehoe lava flow, with very little grass and moss, which was erupted in 1729 (as part of the 1724–1729 events) and fills a large area south of Leirhnjukur (Saemundsson, 1991).

In the small South-Leirhnjukur area, measurements have been made of all observable tectonic fractures at many places along strike, regardless of their size, so that the exact geometry of each fracture could be determined (Fig. 6). In order to define the local fracture orientation, numerous measurements of strike and dip were made along the six main fracture zones and about fifty minor fissures (Fig. 7). No significant tilting has affected the Holocene lava flow, which results in simpler fracture dip estimates.

Concerning the motion vectors across fissures, measurements of the direction of opening were made (using a

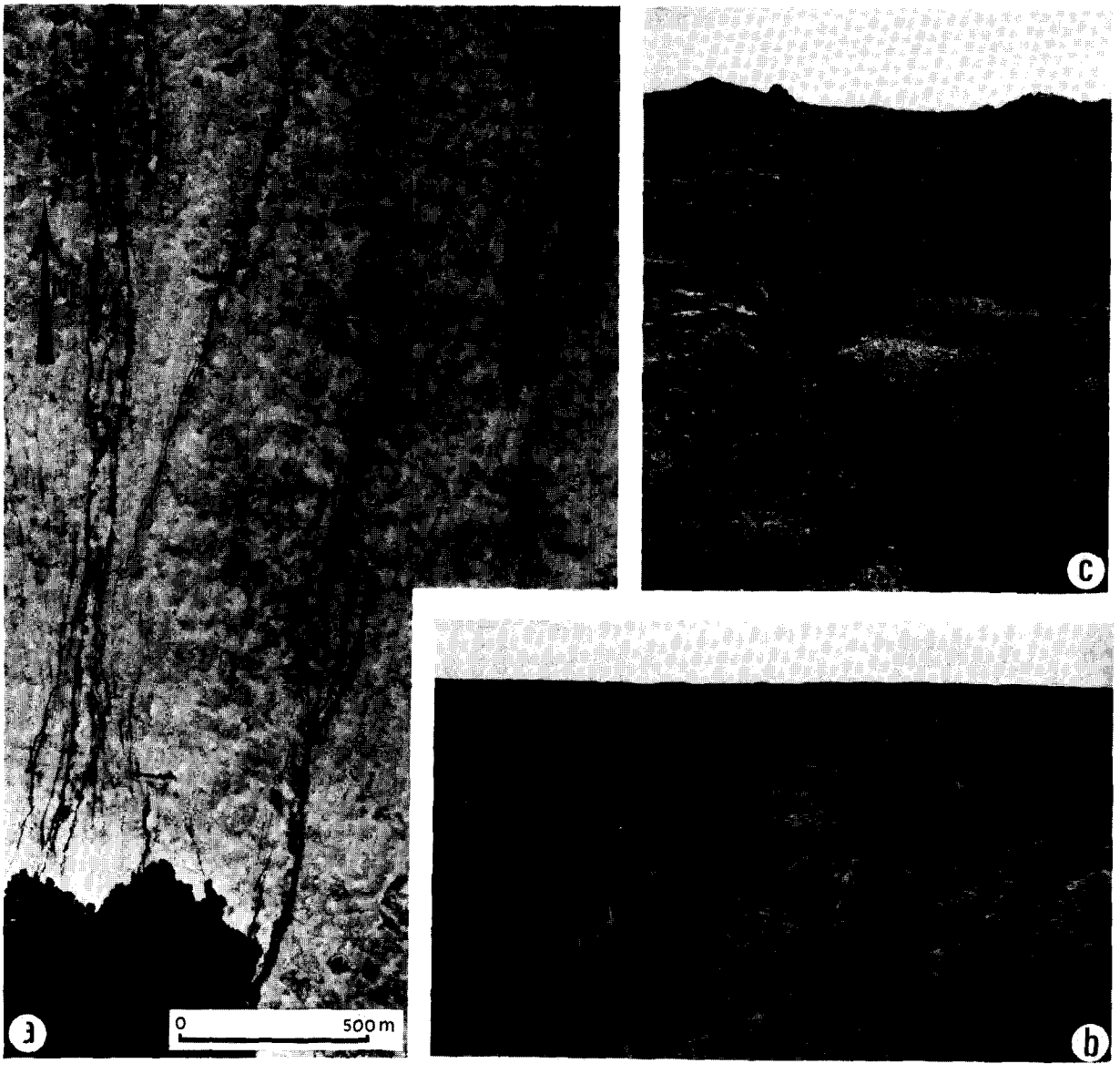

Fig. 4. (a) Aerial photograph of a segment of the Krafla fissure swarm, in the Mófell area, taken on 22 September 1985 (ref. number J5497); fractures lines and recent lava flow black in white snow. (b) View of a graben-like structure, 10–20 m wide, along a major scarp of the Mófell–Hrutafjöll area (compare with Fig. 3c). (c) View of a minor open fissure, 0.5–1 m wide, same area.

Topochaix compass) at 18 locations for 11 fractures. This direction of opening (O–O′ in Fig. 6) was measured at all places where the fit between fracture rims could be reconstructed and the displacement vector obtained by matching wall-rock irregularities. The average direction of opening is N88°E ± 18°, perpendicular to the average strike of fractures. This shows that there is no significant lateral displacement along these fractures. 122 measurements of transverse horizontal dilation, Δe, were made (with a metric tape).

A complete topographic survey of this area was also carried out, with 222 geodetic points distributed in 12 profiles roughly perpendicular to fracture trends (Fig. 7). The determinations of scarp heights, Δv, were part of the geodetic survey. The geometric characteristics of the fractures observed, illustrated in Fig. 6, combine vertical offset (Δv, in the absence of erosion) and dilation (Δe).

As many as 15 open fractures occur on each cross-section (Fig. 7a), with the dilations on individual fractures ranging from a few tens of millimetres to about 1 m. Although some of these fractures result from pure horizontal opening, most of them display vertical offsets (as shown in Figs 3d, 4b & 6). Most fractures trend N–S and correspond to the type illustrated in Figs 3(d) and 4(c). As pointed out before, their direction of extension is generally perpendicular to their trend (Fig. 7a), indicating E–W extension and no significant lateral component of motion.

For all the geodetic measurements, we used a tacheometer 'Topcon GTS 3B20' located at the southern end of the graben (Fig. 7a). The use of this instrument results

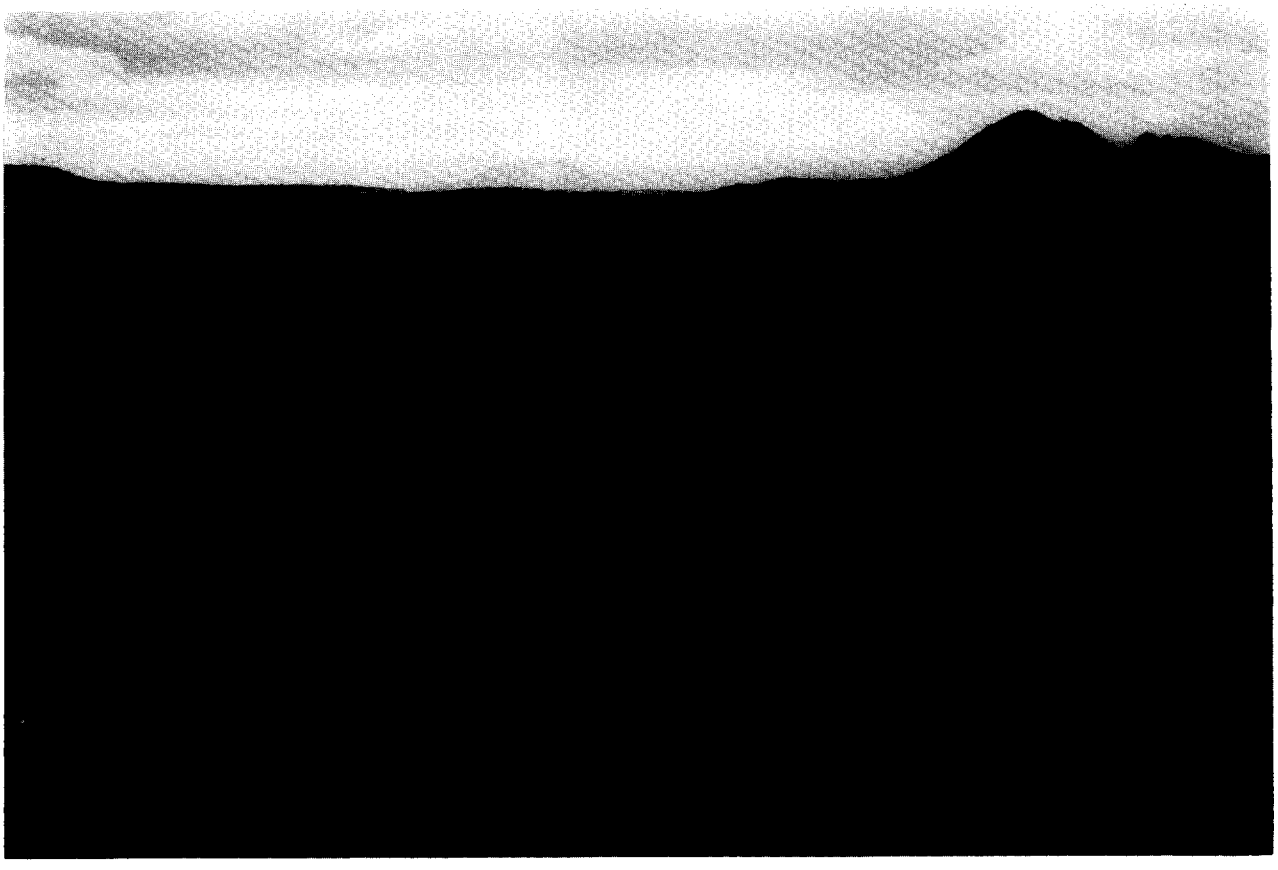

Fig. 5. Photograph of the area studied in detail, taken at its northern end from the volcanic hill Leirhnjukur towards the SSE. On right, black: aa lava flow of the 1984 eruption. Grey, both near the lower-right corner and at the distance on right: pahoehoe lava flow of the 1729 eruption. Covered by grass and cut by fractures: flat top surface of the older lava flows, earliest Holocene in age (about 10,000 years old). Ages of lava flows from Saemundsson (1991).

in an average accuracy of ± 5 mm $+ 3$ ppm for distance measurements ($\Delta L = 5 \times 10^{-3} + 3 \times 10^{-6} L$, where L is the uncertainty and ΔL the length, in metres), and ± 7 seconds for the angles. The distances range from 20 to 260 m. For such short distances, the uncertainty due to angle measurements is small (less than 50%) compared with that due to length measurements. For horizontal distances, most of the uncertainty thus results from the distance measurements. The error in the horizontal location of the points is therefore less than 10 mm. Because most measured segments are short and nearly horizontal, the vertical component of length uncertainty is very small compared with its horizontal component, so that the uncertainty in vertical measurements depends mostly on the uncertainty in angle measurements. In these conditions, the uncertainty in the vertical measurement at a distance of 250 m averages 4 mm. As a consequence, the accuracy in z-values is higher than that in x- and y-values (the uncertainty Δz is always less than 5 mm). The accuracies in horizontal and vertical coordinates are thus sufficiently high, taking our aims into account, and the errors are negligible with respect to other sources of uncertainty (especially those related to dilation measurements across fissures).

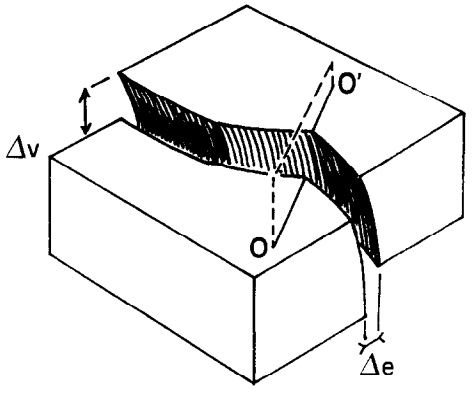

Fig. 6. Measured parameters of fracture displacement. Δv = vertical offset, Δe = transverse horizontal dilation, O–O' = trend of fracture opening (displacement vector reconstructed by matching wall-rock irregularities).

Instrumental uncertainties are negligible for height measurements and are less than 10 mm for dilation estimates. Difficulties in observation produce larger errors, which include the thickness of grass (for the scarp height determination based on comparison between geodetic points), and some problems of fracture rim identification (for dilation estimates). In addition, along five profiles (III to VII), no reliable estimate of

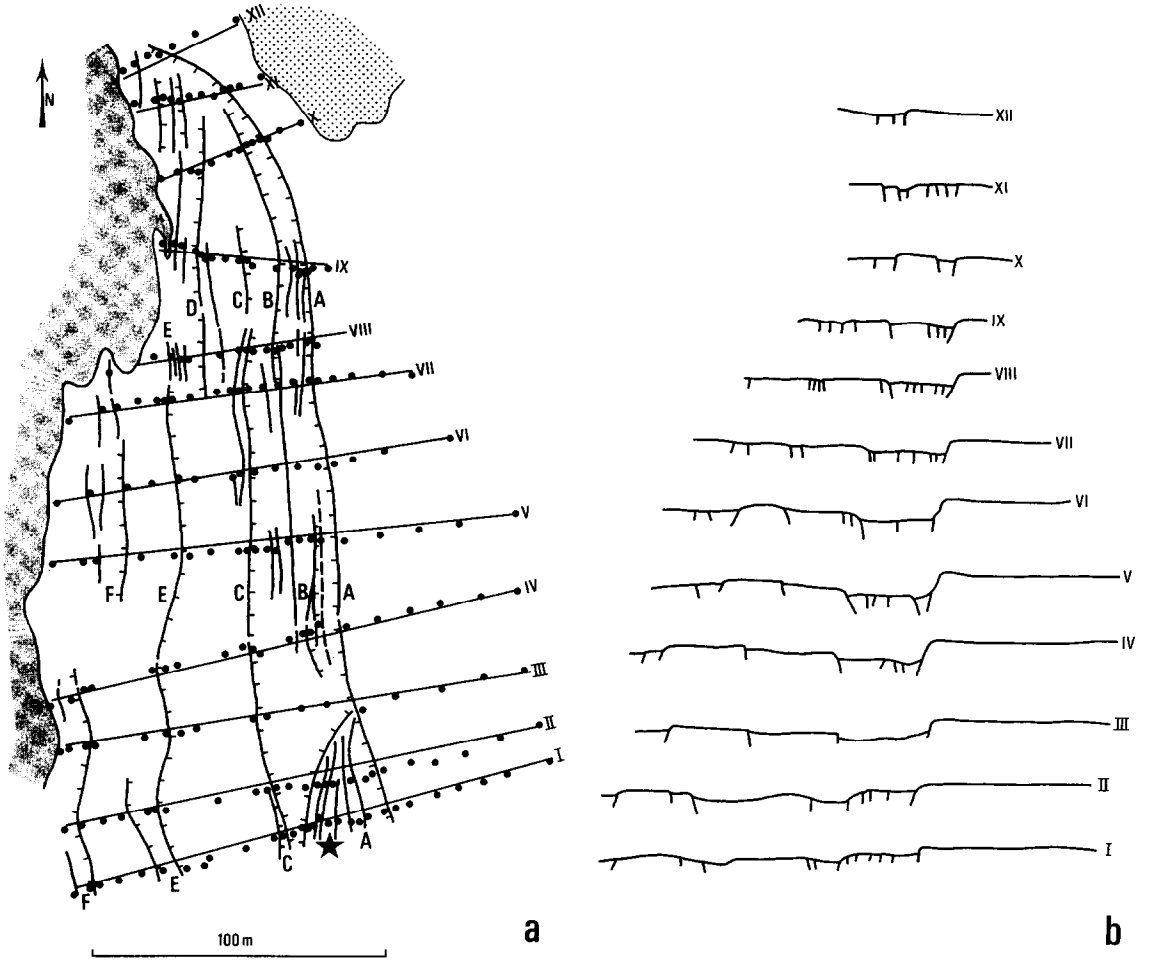

Fig. 7. Results of geodetic survey. (a) Location of geodetic points and main fractures (small dots indicate geodetic points along profiles numbered I to XII, with black star showing the location of the tacheometer); main lava flow top surface left white, younger pahoehoe and aa lava flows in light and dark dotted patterns (respectively); fractures as thin lines (barbs added on the downthrown side where vertical offset is present); A–F refer to scarps mentioned in text. (b) Topographic profiles, numbered I to XII as in (a), with fractures added. Compare with Figs 5 and 8.

transverse horizontal opening across the major eastern fracture could be made because of fallen rocks at the foot of the scarp.

The area mapped in the South-Leirhnjukur is approximately 280 m long and 150 m wide (Figs 7 & 8). Although measurements were collected on individual fractures, the geometrical analysis presented here deals with each fault taken as a whole (A–F, see Fig. 9a), where both the sum of the vertical offsets (as indicated by scarp heights, see Table 1) and the sum of the individual fracture dilations (Table 2) are considered. These fracture zones are typically 5–20 m wide and fit the scarp zones defined in Figs 8 and 9, and mapped in Fig. 7, fairly well.

The shape of each individual fracture was recorded and the components of separation were also measured (Fig. 6). Because blocks often fall from open fracture edges, widening the fissures, measurements of dilation were restricted to fractures showing a good fit between walls. In the area shown in Fig. 5, most dilations are smaller than 1 m, so that no major difficulty was caused by blocks falling from fissure walls (contrary to the Mófell case).

Table 1. Estimates of scarp height, Δv (values in metres). The lines correspond to the five graben sectors located in Fig. 7 (I–XII, reference numbers of profiles). The columns refer to the six fracture zones (A–F) defined in Fig. 7. (1) wide fracture zone

	A	B	C	D	E	F	Total
I–II	5.38 (1)		1.58		2.25	1.94	11.15
III–V	7.32	0.91	2.80		1.22	2.07	14.32
VI–VII	5.68	0.60	1.40	0.40	1.14	1.39	10.61
VIII–IX	3.05	0.64	0.82	1.13	0.42	0.31	6.37
X–XII	1.30	0.45		1.78	0.58		4.11

The deformation of the top surface of the main lava flow is characterised by the presence of a graben (Figs 5 & 8). This graben is bound by two continuous main fault scarps, referred to as A–F in Fig. 7 (from east to west). The east scarp, A, is locally higher than 7.5 m and faces west. On the opposite side of the graben, the height of the east-facing scarp, E, is generally less than 2.5 m. To the south, the eastern, west-facing scarp, A, is divided into 6–7 fractures. The distribution of these scarps is shown in

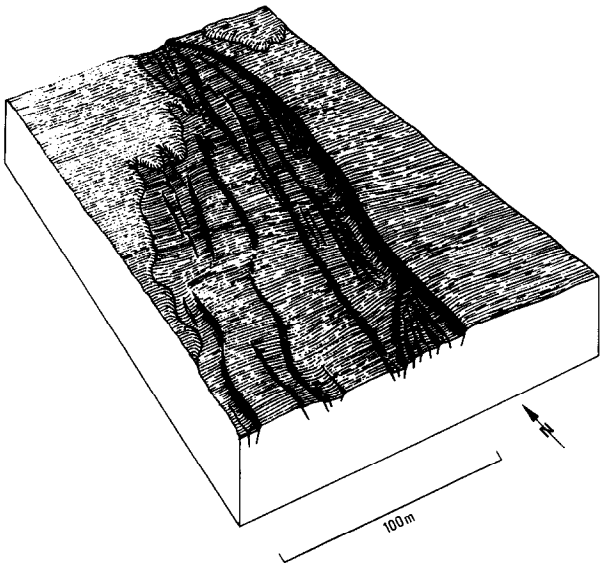

Fig. 8. Schematic view of the area studied, from its southwestern corner towards the northeast. Drawn from map and profiles of Fig. 7. Compare with the photograph of Fig. 5 (taken from the north). Above the flat top surface of the Holocene lava flow are recent lava flows (NW and NE corners).

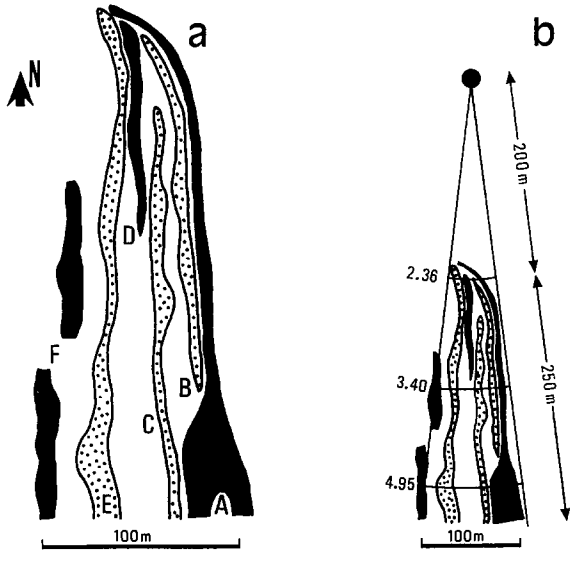

Fig. 9. Horizontal deformation of the area studied. (a) Definition of main scarp-fracture zones (noted A–F, from east to west, as in Fig. 7a); black and dotted zones refer to west-facing and east-facing scarp-fracture zones, respectively. (b) Estimates of average total transverse dilations (values in metres) for three sectors, and the location of the pole of rotation between major blocks east and west of the graben-like fracture system (see text for details).

detail in Fig. 7, and summarised in Fig. 9 (a). At the foot of the major eastern scarp, A, there are two smaller east-facing scarps, B and C. There is also one small west-facing scarp, D, at the foot of the major western (east-facing) scarp, E. In addition, a west-facing scarp, F, is present to the west, outside the graben. This kind of morphology is common, often at a larger scale, such as for the main graben boundary fault scarps in the Krafla fissure swarm (Opheim and Gudmundsson, 1989; Gudmundsson and Bäckström, 1991) and the Thingvellir fissure swarm of southwestern Iceland (Gudmundsson, 1987b).

Table 2. Estimates of fracture zone dilation, Δe (values in metres). The lines correspond to the five graben sectors located in Fig. 7 (I–XII, reference numbers of profiles). The columns refer to the six fracture zones (A–F) defined in Fig. 7. (1) wide fracture zone. (2) values of dilation across zone A obtained from interpolation between I–II and VIII–IX

	A	B	C	D	E	F	total
I–II	2.82 (1)		0.90		0.90	0.33	4.95
III–V	2.09 (2)	0.60	1.31		0.13	0.42	4.55
VI–VII	1.35 (2)	0.18	1.30	0.05	0.32	0.20	3.40
VIII–IX	0.90	0.58	0.60	0.60	0.72	0.05	3.45
X–XII	0.42	0.38		0.94	0.62		2.36

The estimates of scarp heights, Δv, and fracture dilation, Δe, for the six fracture zones (A–F), are summarized in Tables 1 and 2, respectively. Adjacent profiles have been grouped in five main sectors (profiles I–II, III–IV–V, VI–VII, VIII–IX and X–XI–XII: see Fig. 7). The results are consistent for both the heights and the dilations, and provide a basis for the geometrical analysis.

A MODEL FOR SURFACE DEFORMATION AND STRUCTURE AT DEPTH

The geometrical analysis allows accurate reconstruction of a deformation model for the South-Leirhnjukur site. As Table 2 and Fig. 9 show, the total dilation related to the development of the graben shown in Fig. 8 averages 3.7 m and increases from north (about 2 m, sections X–XII) to south (about 5 m, sections I–II). The width of the fracture zone (Fig. 9a) also increases from north (about 30 m and less) to south (about 100 m and more). In the areas on both sides of the graben shown in Figs 5 and 7, the deformation is negligible. First, a large flat area east of the graben is not dissected by fractures (Fig. 5). Second, the area west of the graben is mostly covered by the 1984 aa lava flow (Figs 5 & 7a), but observations at the southwestern corner of the area suggest that it has only minor deformation near the graben.

In the graben, the southward increase of the total dilation reflects the increase in width of the extensional fracture system (Fig. 7, compare with Fig. 3b; see also Figs 5 & 8). Comparing the total dilations in sectors I–II, VI–VII and X–XII (Table 2) and the corresponding widths of the fracture system (about 100 m, 85 m and 30 m; Fig. 9b), the coefficients of extension do not significantly differ (5%, 4% and 7%) while the amount of extension increases southwards.

The length of the studied area averages 250 m (as measured along fracture trends, see Fig. 9a). Assuming rigid block rotation, a pole of rotation can be identified

located approximately 200 m north of the northern tip of the fracture system (Fig. 9b), consistent with the rapid decrease of both the amount of extension and the graben width near this tip. This implies clockwise rotation of the western block relative to the eastern one of 0.6°–0.7°. The studied area is effectively located near the northern tip of one of the extensional fissure sub-systems of the active Krafla fissure swarm. Further south, the total amount of extension related to this particular sub-system is larger than 5 m (the largest value in the area studied), for a width of more than 100 m.

An important aspect in the present study is the subsurface structure as inferred from the active deformation at the surface. Systematic data collection was carried out in terms of lava flow attitudes, fissure orientations and displacement vectors across fracture zones in the portion of the fissure swarm studied. It revealed that both the block rotations and the strike-slip movements are absent, or play a negligible role in terms of overall deformation affecting the pattern of rigid blocks. As a consequence, a complete reconstruction of horizontal dilations and vertical offsets at the surface of the fissure swarm has the potential to reveal the total deformation that has affected the lava pile since about 10,000 years ago, in terms of both the amplitudes and the structural style.

The relationship between the scarp heights, Δv (Table 1), and the dilations across the fracture zones, Δe (Table 2), is illustrated in Fig. 10. It should be noticed that these data were collected at various places along fracture strike, nevertheless excluding fracture tips where relative uncertainties are larger because measured values are small and complex patterns of multiple small open fractures are present. Error bars are added based on individual estimates of the observation errors. Dispersion occurs, especially for low values of scarp height, mostly because of the presence of fractures with predominantly horizontal opening. The distribution shown in Fig. 10 suggests, however, that there is an approximately linear relationship between Δv and Δe, that is, $\Delta v/\Delta e \simeq 3$. In Table 3, the sums of scarp heights and the sums of fracture dilations are listed for each of the five sectors of the fracture system, and their ratios are calculated, resulting in consistent values of about 2.5 for $\Delta v/\Delta e$, which is similar to the distribution in Fig. 10. Despite the large scatter of individual fracture data (Fig. 10), acceptable standard deviations are obtained for each fracture zone (Table 3). This indicates that although large geometrical variations in individual fracture behaviour occur, there is a significant consistency as far as each fracture zone is considered as a whole.

Based on this approximate proportionality, a simple model of the relationships between open fracture geometry observed at the surface and normal fault dip inferred at depth is illustrated in Fig. 11. Two cases are common in the fissure swarms of Iceland: the single scarp structure (Fig. 11a) prevails for small fractures, whereas the graben-like structure (Fig. 11b) dominates where

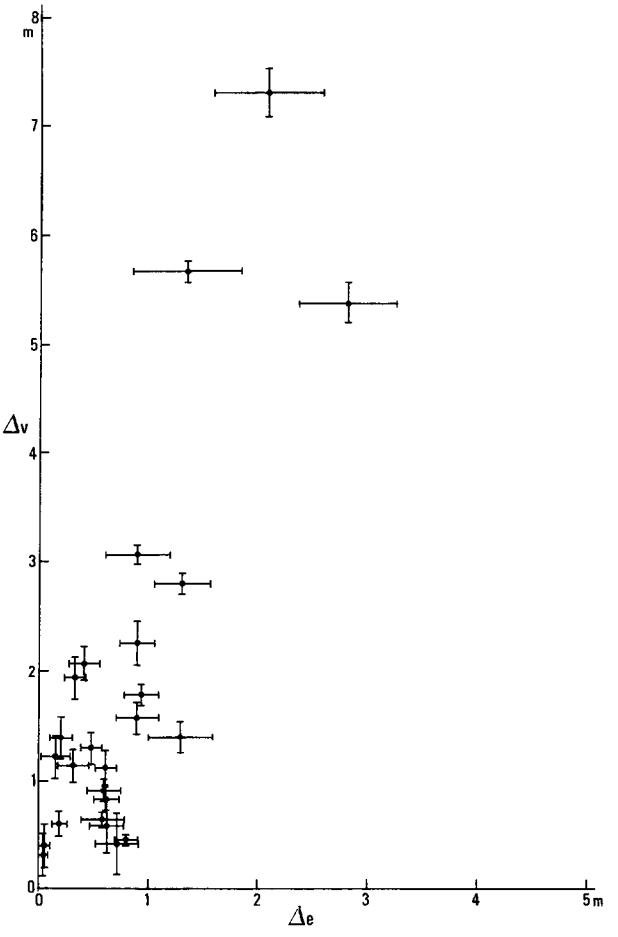

Fig. 10. Graph of the relationship between average scarp heights (Δv) and average dilations (Δe), with error bars. Values in metres, measured at different locations along strikes, for all the fracture zones of Fig. 7.

Table 3. Estimates of the ratio between scarp height, Δv, and fracture zone dilation, Δe. Values of Δv and Δe in metres, with standard deviation added, for the five graben sectors located in Fig. 7 (I–XII, ref. numbers of profiles). ζ is the angle given by $\tan\zeta = \Delta v/\Delta e$ (see text for details), in degrees, with standard deviation calculated

	Δv	Δe	$\Delta v/\Delta e$	ζ
I–II	11.15±0.75	4.95±0.90	2.25±0.56	66±6
III–V	14.32±0.60	4.55±1.20	3.15±0.96	72±5
VI–VII	10.61±0.90	3.40±1.15	3.12±1.32	72±8
VIII–IX	6.37±0.90	3.45±0.95	1.85±0.77	62±11
X–XII	4.11±0.55	2.36±0.50	1.74±0.60	60±9

offsets are large (see also Fig. 3b & c). According to the geometrical analysis illustrated in Fig. 11, the following relationships between Δv, Δe and the dip of the normal fault at depth, ζ, are established as a first approximation:

$$\tan\zeta = \Delta v/\Delta e$$

for the single scarp model (Fig. 11a);

$$\tan\zeta = (\Delta v - \Delta v')/(\Delta e + \Delta e')$$

for the asymmetric graben model (Fig. 11b).

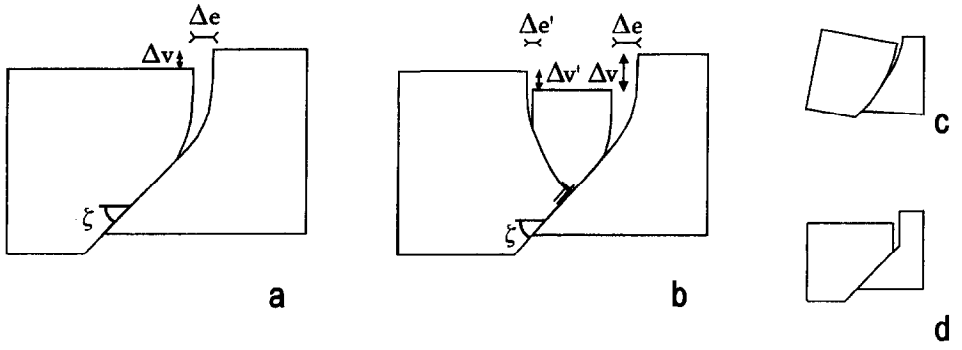

Fig. 11. Models for the relationships between open fracture geometry at the surface and normal fault dip at depth. Δv = scarp height. Δe = fracture dilation. ζ = fault dip. See equations in text. (a) Single-scarp model. (b) Asymmetric graben model. (c) Listric fault geometry. (d) Planar fault geometry (with abrupt change from vertical open fissure near the surface).

Although a single open fracture corresponds to each scarp in the schematic cross-sections of Fig. 11, the actual geometry of fissures is commonly more complex. Numerous open fractures may be present in a single scarp and merge laterally and at depth. In such a case, it is worthwhile to compare the total scarp height, $\Sigma\Delta v$, and the sum of individual fracture dilations in the fracture zone, $\Sigma\Delta e$. One obtains, for the two cases discussed above (respectively):

$$\tan\zeta = \Sigma\Delta v / \Sigma\Delta e, \text{ and}$$
$$\tan\zeta = (\Sigma\Delta v - \Sigma\Delta v')/(\Sigma\Delta e + \Sigma\Delta e').$$

In the South-Leirhnjukur case, the asymmetric graben model is applicable: $\Sigma\Delta v$ and $\Sigma\Delta e$ refer to the sums for all the west-facing scarps while $\Sigma\Delta v'$ and $\Sigma\Delta e'$ refer to sums for all the east-facing scarps. Numerical application with the data of Table 3 yields values of ζ ranging from 60° to 72°, with standard deviations ranging from 5° to 11°. Considering the various sources of uncertainties, as well as the extent of the assumptions made, these values are homogeneous. In the South-Leirhnjukur area (Figs 5 & 8), the deformation of the top surface of the Holocene lava flow therefore indicates the presence at depth of a normal fault which dips 66° ± 8° to the west and corresponds to the main, west-facing scarp, A (Fig. 7).

It is worthwhile to consider the range of possible shapes for the inferred normal faults at moderate depths. The end members are listric (Fig. 11c) or planar (Fig. 11d). Note first that whether the transition from nearly vertical open fissure to inclined normal fault at depth occurs abruptly or progressively does not affect the calculation of the dip of the normal fault at depth as discussed above. According to Opheim and Gudmundsson (1989), listric shapes of faults (Fig. 11c) are uncommon in the Krafla fissure swarm. This observation is in agreement with the presence of vertical cooling joints in basalt flows, because near the surface most open fissures followed these earlier joints. In addition, the absence of—or very minor amounts of—tilting affecting the blocks under consideration favours the interpretation in terms of planar faults (Fig. 11d). A marked listric shape at shallow depths would have resulted in significant block tilting (Fig. 11c). We conclude that an abrupt change from vertical open fissures near the surface to normal faults dipping 60°–72° at moderate depths is more likely.

Estimates of scarp heights and total dilation were made across the five major fracture zones of the Mófell area (Figs 2b & 4a). Five profiles with 450 geodetic points and 93 measurements of fissure dilations were used. With average vertical offsets of 4–12 m and corresponding cumulative dilations of 3.5–9.5 m, the angle ζ averages 51°, based on the same simple geometrical models as before. It is interesting to observe, however, that the range of values obtained for the angle ζ is compatible with that of the South-Leirhnjukur site. The accuracy is poor (extreme values are 23° and 74°). The analysis of the Mófell fracture swarm deserves more geodetic work in the field and therefore is not presented herein.

Further studies may enable these values of ζ beneath major fractures throughout the Krafla fissure swarm to be constrained more closely. It may also enable one to determine whether the minimum bound for fault dip value simply results from large uncertainties, or may reflect an excess of dilation as we suspect based on observation of large fissures with little vertical offset. This excess of dilation may result from systematic fracture opening related to dyke injection at shallow depth. Detailed estimates of extensional deformation across the whole fissure swarm should consider separately the contribution of open fractures principally related to normal shear at depth, as shown by scarps bounding large blocks at the surface (Fig. 3a), and that of pure tension fissures inside the blocks.

DISCUSSION

The subsurface structure of the axial rift zone of NE Iceland (Fig. 1) is poorly known, because of the continuous infill by recent lava flows and the absence of significant erosion. It is worthwhile to check the model of relationships between surface fissure opening and deeper

deformation presented above. It is thus appropriate to analyse not only the present-day axial rift, but also some domains which occupied an equivalent position and underwent similar deformation in the past, because their later erosion allows observation of structure at moderate depths. The uplift and erosion of the present rift shoulders, which corresponded to the axial rift zone in the past, provide easy access to deeper structures of the brittle crust. Sections of volcanic piles are observable in the flanks of deep valleys eroded by glaciers and correspond to ancient rift zone infills which have drifted away from the divergent plate boundary, and been uplifted and eroded. Because no drastic change in oceanic rifting process has occurred in Iceland since the Middle–Late Tertiary, one may infer that the structures observed in the Late Tertiary volcanic piles are quite similar to those developing beneath the present axial rift zone. The depth of erosion in the oldest volcanic areas of Iceland (located in Fig. 12), where the lava pile is 10–16 Ma old, commonly reaches 1–2 km (Walker, 1974; McDougall *et al.*, 1984).

Figure 12 summarises the distribution of 1169 dip measurements collected on normal faults, major and minor, in the oldest volcanic areas, where extensive fault slip analyses were carried out. These are the Vestfirdir peninsula of NW Iceland (Gudmundsson *et al.*, 1996) and the coastal area of eastern Iceland (Bergerat *et al.*, 1990). Back-tilting was done where appropriate; it is generally unnecessary because most tilted blocks have dips of only a few degrees. The frequency diagrams corresponding to these dip-slip normal fault data clearly show that the most common dips fall in the range from 60° to 80°. Such observations were made throughout Iceland, consistently revealing that normal faults related to rift extension usually dip 70° ± 10°. In the active Krafla fissure swarm, based on studies of surface deformation using simple models (Fig. 11), we obtained a value of 66° ± 8° for the subsurface dips of normal faults. This value based on detailed local reconstruction at the South-Leirhnjukur site falls within the range of the rough estimates obtained from the active Mófell fissure swarm. Our conclusion that surface extension in the active rift is accommodated by normal faulting at depth, and that normal faults dip approximately 60°–75°, is thus consistent with the results of independent geological observations and statistical analysis carried out within the deeper volcanic formations in the rift shoulder zones (Fig. 12).

The extension at the surface of the axial rift zone of NE Iceland is mainly characterised by fissuring, in the absence of fluid pressure (see upper section, a, in Fig. 13). Such predominant tension crack opening results in the development of spectacular fissure swarms (Fig. 4a). A vertical component of displacement is often also present. Careful estimates of the vertical offsets and total horizontal dilation across fracture zones, despite difficulties related to complex patterns such as for graben-like structures, generally yield consistent ratios which indicate that these fracture zones, where vertical displacement between large blocks occurs as well as extension, are underlain by normal faults (Fig. 11), and that these normal faults dip 60°–75° (see middle section, b, in Fig. 13).

Pure horizontal dilation can occur. Near the surface, it results in horizontal opening of vertical open cracks, and in fissure eruptions. At depth, it is accounted for by dyke

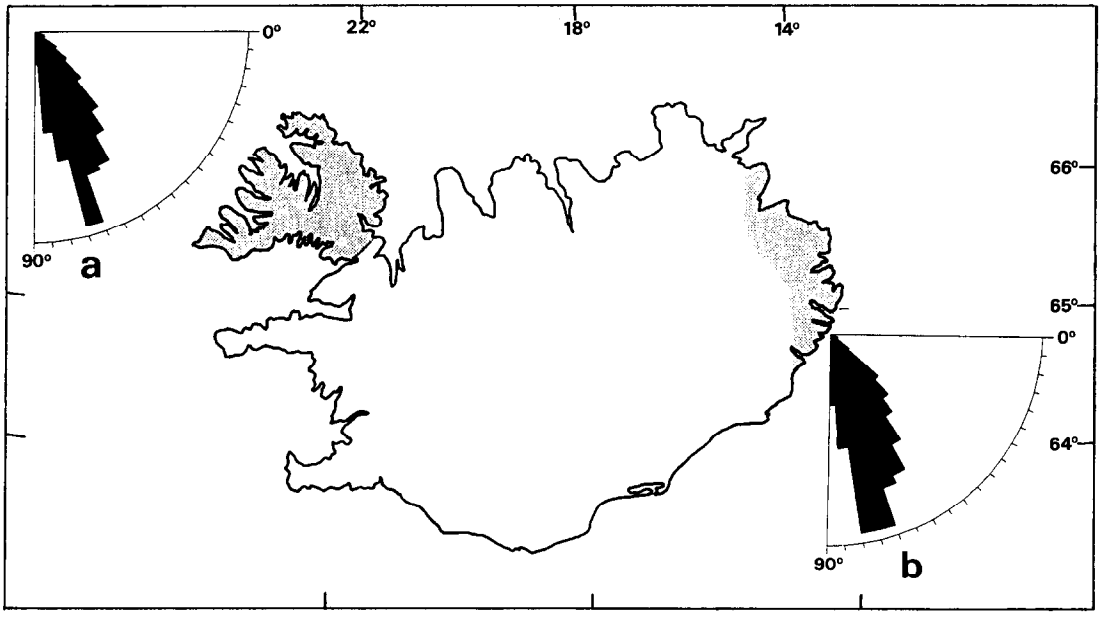

Fig. 12. Distribution of the dips of normal faults measured in the oldest, deeply eroded zones of the rift shoulders in Iceland (shaded areas in map). (a) Vestfirdir peninsula of northwestern Iceland, 836 fault data at 87 sites (from Gudmundsson *et al.*, 1996). (b) Eastern coastal area of Iceland, 333 fault data at 48 sites (Bergerat *et al.*, 1990).

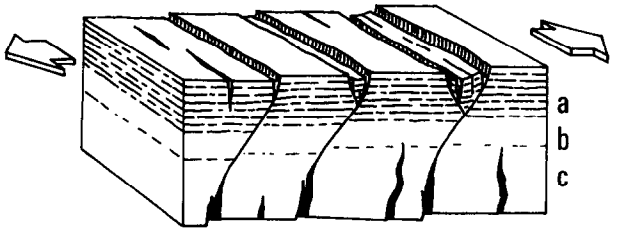

Fig. 13. Schematic distribution of the tension and shear in the young upper brittle crust of the rift zone in Iceland. a—upper section with open fractures and fissure swarms (actual tension near the surface, with low lithostatic pressure). b—middle section where normal shear (normal faulting) prevails (increasing lithostatic pressure, moderate fluid pressure). c—section with both dyke opening (high magmatic pressure resulting in effective tension despite lithostatic pressure), and normal faulting. Note that the relationship between normal faults and dykes is hypothetical and very rarely observed in the Tertiary lava pile (Forslund and Gudmundsson, 1991).

injection, which is well documented from studies on rift shoulders, where eroded lava flow piles are cut by numerous dykes. Field work showed that dyke injection and normal faulting are commonly associated in Iceland (Gudmundsson, 1995b). According to a model of dyke injection with instantaneous emplacement of a dyke at a shallow depth below the Earth's surface, dyke injection should induce formation of a graben above it at the surface (Pollard and Holzhausen, 1979). However, the size of the graben generated above a dyke should be small according to Bonafede and Olivieri (1995). Modelling by Rubin and Pollard (1988) also predicts little subsidence above the subsurface dyke top. Field observations in Iceland show that dyke emplacement does not necessarily lead to the development of such a graben (Gudmundsson, 1995b). In order to simulate the surface effect of a growing dyke, analogue experiments were performed by Mastin and Pollard (1988). Their results indicate that (1) to generate tension fractures, the top of a dyke with a 'blunt end' must be at a depth less than about ten times the thickness of the dyke, and (2) to produce normal faults, this depth must be less than about five times the thickness of the dyke near its top. For instance, based on observations in the Krafla area, Gudmundsson (1995b) computed that a 1 m thick magma injection had to be within 10 m from the surface to generate fissures, and within 5 m to generate a graben. Because the width of this graben is nearly equal to the depth to the top of the dyke generating it (Mastin and Pollard, 1988), the resulting graben in this case should be about 5 m wide (Gudmundsson, 1995b). Because most dykes do not have 'blunt ends', these depths could be even shallower, and the dyke would normally be a feeder. In addition, Gudmundsson (1995b) considers that where a vertically propagating dyke enters a graben, the magmatic overpressure that accompanies dyke injection may tend to lock the graben faults adjacent to the dyke. Observations in the fissure swarms of northeastern Iceland suggest that normal fault scarps or grabens and dyke injection are both the result of the same plate-tectonic loading conditions and thus are commonly generated simultaneously during rifting episodes.

We infer that despite the common presence of normal faults and grabens at the Earth's surface, pure dilation plays an important role at greater depths, because of dyke intrusion (see lower section, c, in Fig. 13). Normal faulting co-exists with dyke emplacement and plays a significant role in the deepest section of the upper brittle crust. Concerning the present-day tectonics, this is shown by the focal mechanisms of earthquakes despite multiple tectonic and volcanic origins (Einarsson, 1991). Analyses of microearthquake swarms with high accuracy relocation of events were recently carried out in the South Iceland Seismic Zone. For some sample faults, at depths of 3–5 km, these seismological analyses revealed dips of about 63° (Slunga *et al.*, 1995) and 72–81° (Rögnvaldsson and Slunga, 1994). These results independently obtained are in agreement with our estimates, but the validity of the comparison is poor because the South Iceland Seismic Zone is a transform zone (not a typical rift segment as for the Krafla area) and most focal mechanisms on these faults are principally strike-slip. More microseismic surveys are thus needed in order to determine the extent and the dip of normal faults at depth. The most reliable confirmation of our normal fault dip estimates is obtained through the comparison with earlier, similar faults observable in rift shoulders. Unfortunately, erosion of the rift shoulders does not reach crustal depths of more than about 2 km so that direct observation at larger depths is not possible.

CONCLUSION

In the axial rift zone of northeastern Iceland, the extensional deformation in the upper crust is localised at all scales, and dominated by two processes, horizontal tension and normal shear (Fig. 13). Tension dominates in the uppermost several hundred metres, because of the presence of the free surface and the small lithostatic pressure, resulting in spectacular fissure swarm development (Figs 2b & 4a). Effective tension plays an important role at depths of 2–5 km and more, as the result of dyke injection from nearby magma chambers. The magmatic fluid pressure in fractures results in effective tension, and the presence of intense dyke swarms in the deep sections of the eroded rift shoulders provides direct evidence that magmatic pressure is large enough to allow injection of magma (Gudmundsson, 1987c, 1995a,b).

Analysis of surface deformation in the active Krafla fissure swarm of the rift zone in northern Iceland suggests that normal shear plays a major role at intermediate depths in the upper brittle crust. As a result, normal faulting occurs along planes which dip 60°–75° on average, at a crustal depth of about 1 km. This occurrence of shear at intermediate depths in the nascent oceanic crust (Fig. 13) corresponds to an equilibrium between the upward decrease in lithostatic pressure

which favours fissure opening at the Earth's surface and the occurrence of effective tension at depth owing to magmatic pressure and dyke emplacement.

Acknowledgements—This work was supported by the French–Icelandic scientific cooperation programme (Iceland Ministry of Education and Culture, and the French Ministère des Affaires Etrangères), and by the D.B.T.-INSU French program (contribution n° 66). We thank the French Embassy in Iceland for help and the Iceland Geodetic Institute for permission to publish Fig. 4(a). We especially thank Águst Gudmundsson for fruitful discussions and suggestions regarding fissure swarms and dykes, and for his help concerning the geological literature in Icelandic. We also thank the referees, Drs D. Peacock and R. Jolly, for thorough correction and constructive comments which resulted in significant improvement of the paper.

REFERENCES

Bergerat, F., Angelier, J. and Villemin, T. (1990) Fault systems and stress patterns on emerged oceanic ridges: a case study in Iceland. *Tectonophysics* **179**, 183–197.

Björnsson, A., Saemundsson, K., Einarsson, P., Tryggvason, E. and Grönvold, K. (1977) Current rifting episode in north Iceland. *Nature* **226**, 318–323.

Björnsson, A., Saemundsson, K. and Steingrimsson, B. (1984) The Krafla eruptions (in Icelandic). *Reykjavik, Iceland, National Energy Autority, Orkustofnun, Report OF-84077/JHD-31b.*

Bonafede, M. and Olivieri, M. (1995) Displacement and gravity anomaly produced by a shallow vertical dyke in a cohesionless medium. *Geophysical Journal International* **123**, 639–652.

De Mets, C. R., Gordon, R. G., Argus, D. and Stein, S. (1990) Current plate motions. *Geophysical Journal International* **101**, 425–478.

Einarsson, P. (1991) Earthquakes and present-day tectonism in Iceland. *Tectonophysics* **189**, 261–279.

Eliason, S. (1979) Kerlingarholar, old eruptive fissures in the Krafla fissure swarm. (In Icelandic, with English summary.) *Naturufraedingurinn* **49**, 51–63.

Forslund, T. and Gudmundsson, A. (1991) Crustal spreading due to dikes and faults in Southwest Iceland. *Journal of Structural Geology* **13**, 443–457.

Forslund, T. and Gudmundsson, A. (1992) Structure of Tertiary and Pleistocene normal faults in Iceland. *Tectonics* **11**, 57–68.

Grönvold, K. (1984) Chemical composition of the lava. *Professional paper* 8401. Nordic Volcanological Institute, Reykjavik, Iceland.

Gudmundsson, A. (1987a) Geometry, formation and development of tectonic fractures on the Reykjanes Peninsula, Southwest Iceland. *Tectonophysics* **139**, 295–308.

Gudmundsson, A. (1987b) Tectonics of the Thingvellir fissure swarm, SW Iceland. *Journal of Structural Geology* **9**, 61–69.

Gudmundsson, A. (1987c) Formation and mechanics of magma reservoirs in Iceland. *Geophysical Journal of the Royal Astronomical Society* **91**, 27–41.

Gudmundsson, A. (1992) Formation and growth of normal faults at the divergent plate boundary in Iceland. *Terra Nova* **4**, 464–471.

Gudmundsson, A. (1995a) Infrastructure and mechanics of volcanic systems in Iceland. *Journal of Volcanology and Geothermal Research* **67**, 1–22.

Gudmundsson, A. (1995b) The geometry and growth of dykes. In *Physics and Chemistry of Dykes*, eds G. Baer and A. Heimann, pp. 23–34. Balkema, Rotterdam.

Gudmundsson, A. and Bäckström, K. (1991) Structure and development of the Sveinagja graben, Northeast Iceland. *Tectonophysics* **200**, 111–125.

Gudmundsson, A., Bergerat, F. and Angelier, J. (1996) Off-rift and rift-zone paleostresses in Northwest Iceland. *Tectonophysics* **255**, 211–228.

Gudmundsson, A. T. (1986) *Islandseldar (Iceland Fires)*. Vaka-Helgafell, Reykjavik.

McDougall, I., Kristjansson, L. and Saemundsson, K. (1984) Magnetostratigraphy and geochronology of Northwest Iceland. *Journal of Geophysical Research* **89**, 7029–7060.

Mastin, L. G. and Pollard, D. D. (1988) Surface deformation and shallow dike intrusion processes at Inyo Craters, Long Valley, California. *Journal of Geophysical Research* **93**, 13221–13235.

Opheim, J. and Gudmundsson, A. (1989) Formation and geometry of fractures, and related volcanism, of the Krafla fissure swarm, northeast Iceland. *Bulletin of the Geological Society of America* **101**, 1608–1622.

Pollard, D. D. and Holzhausen, G. (1979) On the mechanical interaction between a fluid-filled fracture and the Earth's surface. *Tectonophysics* **53**, 27–57.

Rögnvaldsson, S. Th. and Slunga, R. (1994) Single and joint fault plane solutions for microearthquakes in South Iceland. *Tectonophysics* **237**, 73–80.

Rubin, A. M. and Pollard, D. D. (1988) Dike-induced faulting in rift zones of Iceland and Afar. *Geology* **16**, 413–417.

Saemundsson, K. (1974) Evolution of the axial rifting zone in Northern Iceland and the Tjörnes fracture zone. *Bulletin of the Geological Society of America* **85**, 495–504.

Saemundsson, K. (1980) Outline of the geology of Iceland. *26th International Geological Congress Jökull* **29**, 7–28.

Saemundsson, K. (1991) Jardfraedi Kroflukerfisins (Geology of the Krafla volcanic system). In *Nattura Myvatns (Myvatn's Nature)*, eds A. Gardarsson and A. Einarsson, pp. 25–95. Hid Islenska Natturufraedifelag, Reykjavik.

Slunga, R., Rögnvaldsson, S. Th. and Bödvarsson, R. (1995) Absolute and relative locations of similar events with application to microearthquakes in southern Iceland. *Geophysical Journal International* **123**, 409–419.

Tryggvason, E. (1980) Subsidence events in the Krafla area, North Iceland 1975–1979. *Journal of Geophysics* **47**, 141–153.

Tryggvason, E. (1984) Widening of the Krafla fissure swarm during the 1975–1981 volcano–tectonic episode. *Bulletin of Volcanology* **47**, 47–69.

Tryggvason, E. (1986) Multiple magma reservoirs in a rift zone volcano: Ground deformation and magma transport during the September 1984, eruption of Krafla, Iceland. *Journal of Volcanology and Geothermal Research* **28**, 1–44.

Walker, G. P. L. (1974) The structure of eastern Iceland. In *Geodynamics of Iceland and the North Atlantic Area*, ed. L. Kristjansson, pp. 177–188. Reidel, Dordrecht.